SUPPLEMENTAL FIGURES

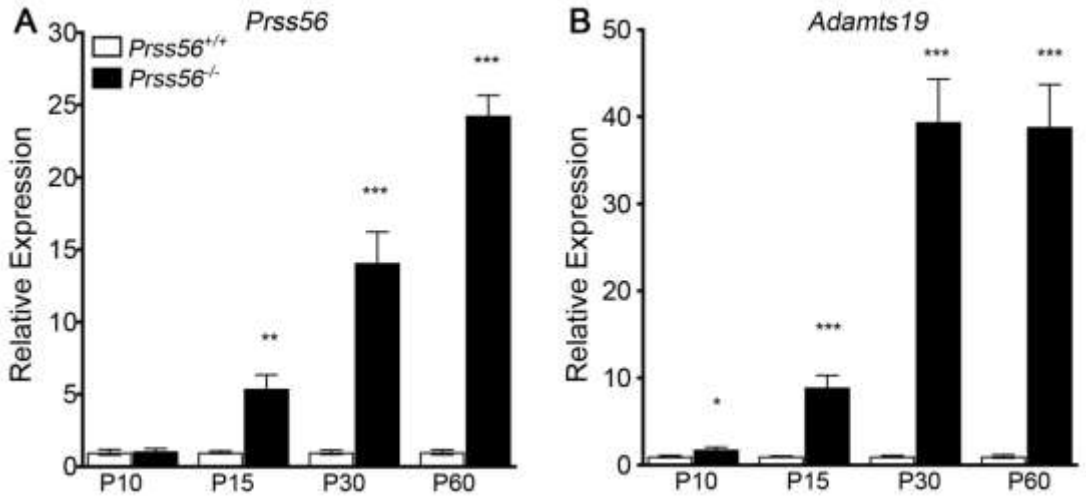

Figure S1. *Prss56* and *Adamts19* expression in *Prss56*$^{-/-}$ retina across ages. (**A**-**B**) Graphs showing quantification of *Prss56 (***A**) and *Adamts19* (**B**) mRNA levels using qPCR in wild-type and mutant retina at different developmental stages. A significant increase in *Adamts19* mRNA levels was detected as early as P10 in *Prss56* mutant retina (**B**), while upregulation in *Prss56* mRNA was first observed at P15 in the mutant retina (**A**). The magnitude of the increase of both *Prss56* and *Adamts19* expression became more pronounced with age in the mutant retina. *Prss56* and *Adamts19* expression were normalized to the expression of three housekeeping genes (*Hprt1*, *Actb1,* and *Mapk1).* Data are presented as fold expression relative to wild-type (mean ± SEM), N=4 to 6/group. *****p<0.05; ******p<0.01; *******p<0.001, t-test. The *Prss56* qPCR data in **A** were previously published in Figure 4 of Paylakhi et al. 2018 [13].

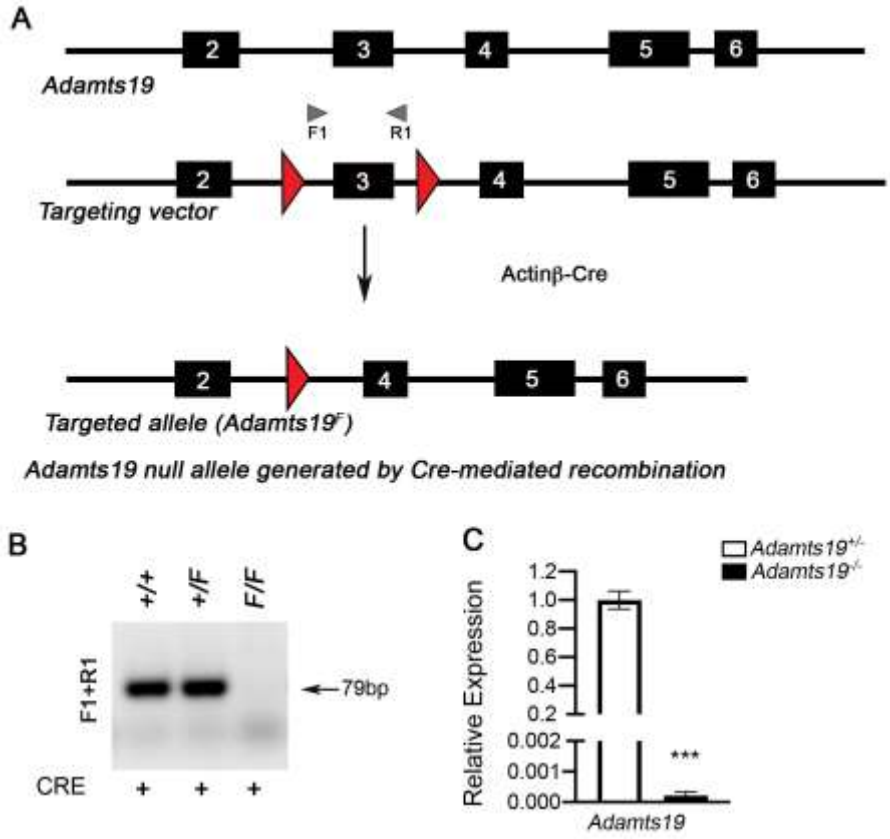

Figure S2. Generation of *Adamts19* mutant mice allele.

(**A**) The LoxP site flanks the exon 3 of the *Adamts19*^{F} allele. In presence of Cre recombinase, the Adamts19 exon is deleted resulting in a frameshift mutation and premature stop codon, rendering the *Adamts19* catalytically inactive. (**B-C**) *Adamts19* exon 3 excisions was confirmed by PCR as well as qPCR. (**B)** PCR amplification of DNA from wild-type (Adamts19$^{+/+}$, lane 1), heterozygous (Adamts19$^{F/+,}$ lane 2), or homozygous (*Adamts19*$^{F/F}$) mice. PCR reactions were performed using primers amplifying regions of intron 2 and exon 3. The deletion of exon 3 from the *Adamts19*$^{F/F}$ allele gives no PCR product. using primers amplifying a region of intron 2 and exon 3 gives no PCR product from DNA from *Adamts19*$^{F/F}$ mice. (**C)** qPCR analysis employing primers amplifying exon 3 of A*damts19* further confirm that Adamts19 transcript from *Adamts19*$^{-/-}$*;Prss56* $^{-/-}$ retina lacks exon 3.

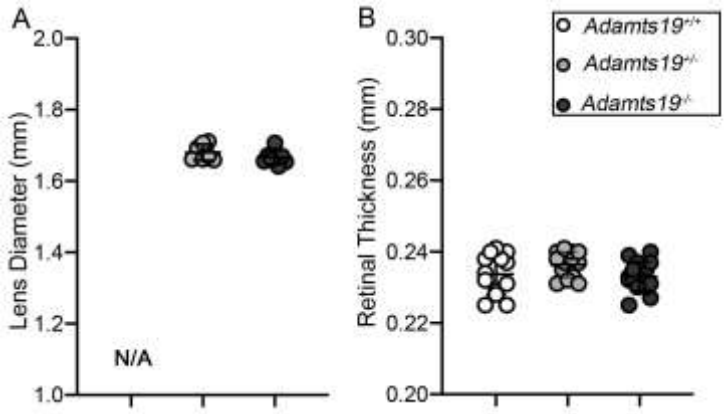

Figure S3. Ocular biometric analysis in *Adamts19* mutant mice

Histograms showing that ocular the lens diameter (**A**) and retinal thickness (**B**) were indistinguishable in *Adamts19*$^{-/-}$;*Prss56*$^{-/-}$, *Adamts19*$^{+/-}$;*Prss56*$^{-/-}$ and control *Adamts19*$^{+/-}$; *Prss56*$^{+/-}$ mice. Data are presented as mean ± SD, N≥7/group. *p<0.05, One-way ANOVA.

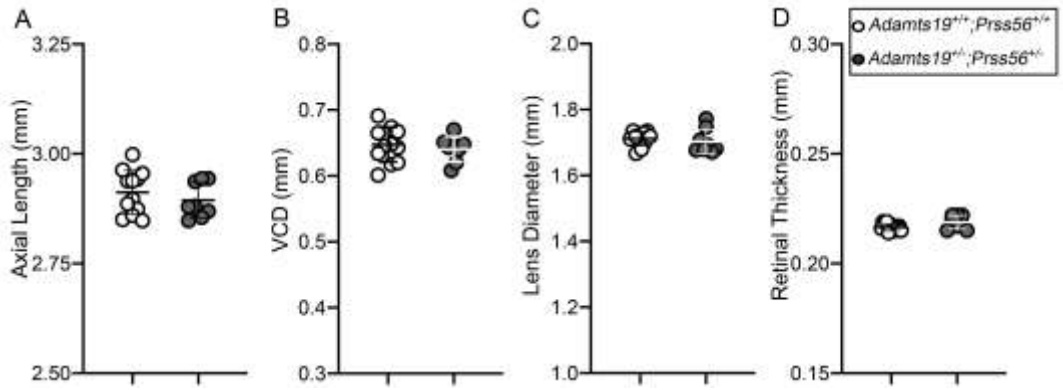

Figure S4. Ocular biometric parameters are indistinguishable between wild-type and *Adamts19$^{+/-}$:Prss56$^{+/-}$* mice. (**A-D**) Histograms showing that all the ocular biometric parameters examined including axial length (**A**), vitreous (VCD) (**B**), lens diameters (**C**) and retinal thickness (**D**) are indistinguishable between wild-type (*Adamts19$^{+/+}$;Prss56$^{+/+}$*) and *Adamts19$^{+/-}$;Prss56$^{+/-}$* mice at P18 Data are presented as mean ± SD, N≥7/group. *p<0.05, One-way ANOVA.

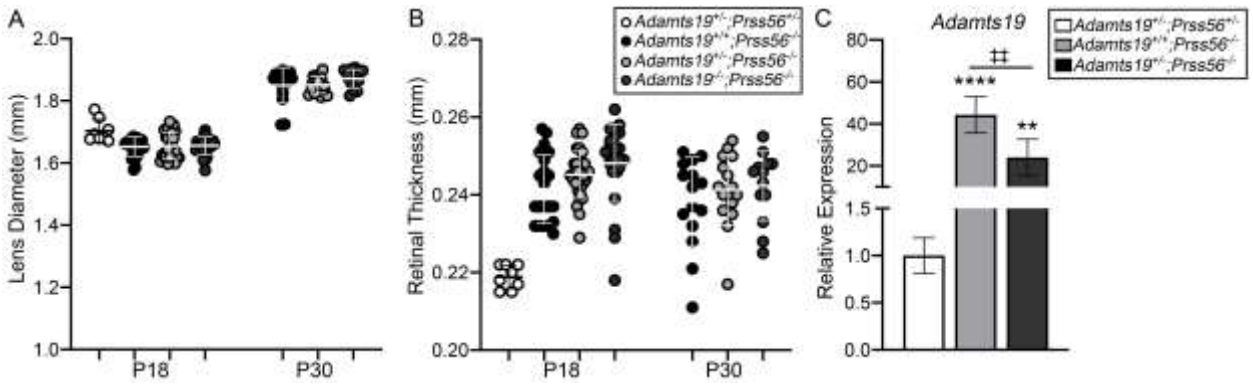

S5. Ocular biometric analysis of *Adamts19$^{-/-}$;Prss56$^{-/-}$* mice. (**A-B**) Histograms showing that retinal thickness (**A**) is modestly increased in *Adamts19$^{-/-}$;Prss56$^{-/-}$* mice compared to control *(Adamts19$^{+/-}$; Prss56$^{+/-}$)* mice at P18, but not at P30, while the lens diameter (**B**) is indistinguishable in *Adamts19$^{-/-}$;Prss56$^{-/-}$*, *Adamts19$^{+/-}$;Prss56$^{-/-}$* and control *(Adamts19$^{+/-}$; Prss56$^{+/-}$)* mice at both ages examined. (**C**) Histogram showing relative *Adamts19* mRNA levels AGE N>4/group. Data are presented as mean ± SD, N≥13/group. *p<0.05, One-way ANOVA.

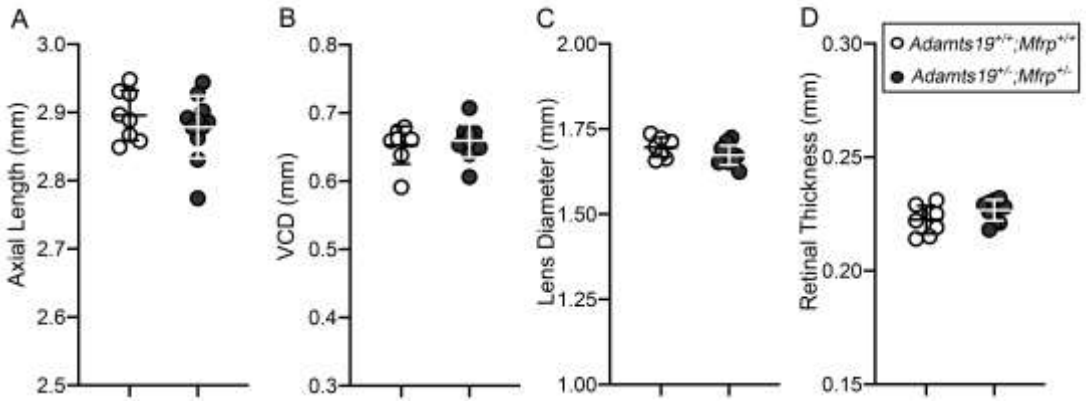

Figure S6. Ocular biometric parameters are indistinguishable between wild-type and *Adamts19$^{+/-}$:Mfrp$^{+/-}$* mice. (**A-D**) Histograms showing that all the ocular biometric parameters examined including axial length (**A**), vitreous (VCD) (**B**), lens diameters (**C**), and retinal thickness (**D**) are indistinguishable between wild-type (*Adamts19$^{+/+}$;Mfrp$^{+/+}$*) and *Adamts19$^{+/-}$;Mfrp$^{+/-}$* mice at P18. Data are presented as mean ± SD, N≥7/group. *p<0.05, One-way ANOVA.

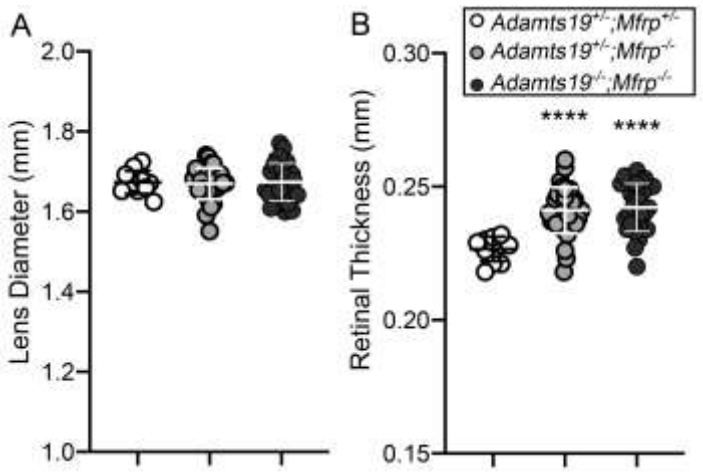

Figure S7. Ocular biometric analysis of *Adamts19$^{-/-}$;Mfrp$^{-/-}$* mice. (**A-C**) Histograms showing that the lens diameter (**A**) are indistinguishable in *Adamts19$^{+/-}$*; *Mfrp$^{-/-}$*, *Adamts1$^{-/-}$*; *Mfrp$^{-/-}$*, and control *(Adamts19$^{+/-}$*; *Mfrp$^{+/-}$*) mice, while the retinal thickness (**B**) is increased in both *Adamts19$^{+/-}$*; *Mfrp$^{-/-}$* and *Adamts1$^{-/-}$;Mfrp$^{-/-}$* mice compared to control *Adamts19$^{+/-}$*; *Mfrp$^{+/-}$* mice at P18. Data are presented as mean ± SD, N≥11/group. ****p<0.0001, One-way ANOVA.

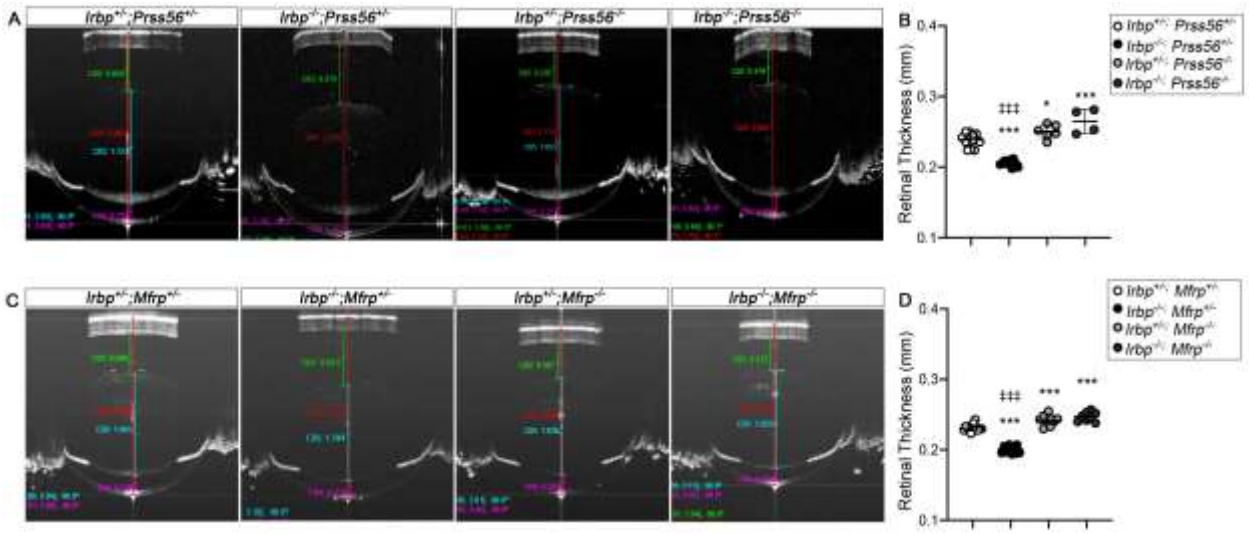

Figure S8.

Ocular biometric analysis of *Irbp* mutant mice following *Prss56* inactivation

(A) Representative OCT images showing that ocular axial length (quantified in Fig. 6A) and VCD (quantified in Fig. 6 B) are increased in *Irpb* mutant mice (*Irpb*$^{-/-}$*; Prss56*$^{+/-}$) and reduced in *Prss56* mutant mice compared to control *Irpb*$^{+/-}$*; Prss56*$^{+/-}$ control mice at P18. In contrast, retinal thickness (**B**) were reduced in *Irpb* mutant mice (*Irpb*$^{-/-}$*; Prss56*$^{+/-}$) and retinal thickness was increased in *Prss56* mutant and *Irbp;Prss56* double mutant mice (*Irpb*$^{+/-}$*; Prss56*$^{-/-}$ and *Irbp*$^{-/-}$*; Prss56*$^{-/-}$, respectively) compared to control *Irpb*$^{+/-}$*; Prss56*$^{+/-}$ mice. Data are presented as mean ± SD, N≥4/group. ******p<0.01; *******p<0.0001 (compared to controls); ‡‡‡p<0.001 (compared to double mutant *Irpb*$^{-/-}$;*Prss56*$^{-/-}$ mice), One-way Anova.

Biometric analysis of *Irbp* mutant mice following *Mfrp* inactivation (**C**) Representative OCT images showing that ocular axial length (quantified in Fig. 6 C) and vitreous chamber depth (VCD, quantified in Fig. 6 D) are increased in *Irpb* mutant mice (*Irpb*$^{-/-}$*; Mfrp*$^{+/-}$) and reduced in *Mfrp* mutant and *Irbp;Mfrp* double mutant mice (*Irpb*$^{+/-}$*; Mfrp*$^{-/-}$ and *Irbp*$^{-/-}$*; Mfrp*$^{-/-}$, respectively) compared to control *Irpb*$^{+/-}$*; Mfrp*$^{+/-}$ mice at P18. In contrast, and retinal thickness (**D**) were reduced in *Irpb* mutant mice (*Irpb*$^{-/-}$*; Mfrp*$^{+/-}$) and retinal thickness was increased in *Mfrp* mutant and *Irbp;Mfrp* double mutant mice (*Irpb*$^{+/-}$*; Mfrp*$^{-/-}$ and *Irbp*$^{-/-}$*; Mfrp*$^{-/-}$, respectively) compared to control *Irpb*$^{+/-}$*; Mfrp*$^{+/-}$ mice. Data are presented as mean ± SD, N≥8/group. ******p<0.01; *******p<0.0001 (compared to controls); ‡‡‡p<0.001 (compared to double mutant *Irpb*$^{-/-}$; *Mfrp*$^{-/-}$ mice), One-way Anova.

Table S1. List of genotyping primers

Allele (mouse strain)	Primer name	Primer sequence
Prss56^{glcr4} **(C57BL/6.Cg-Prss56 glcr4/SjJ)**	Prss56 glcr4 F1	5' TGGCTCCAGAAACCAAAGCCGGAA GAGCGCCCGGAAACAAAGAGT 3'
	Prss56 glcr4 F2	5' GCGGCGCCCGGAAACAAAAGGA 3'
	Prss56 glcr4 R	5' TCCTGGAAGAGAGGGAGTGA 3'
Prss56^{Cre} **(C57Bl/6.Cg-Prss56tm)**	Prss56 Cre F	5' CAG GGC ATC GTT TCC CTG AG 3'
	Prss56 Cre R WT	5' GAC AGG CGC GTG TAC AGT GG 3'
	Prss56 Cre R Cre	5' CCA TGA GTG AAC GAA CCT GG 3'
Egr1$^{-/-}$ **(C57BL/6. Egr1tm1Jmi/J)**	EGR1 common R	5' GGG CAC AGG GGA TGG GAA3
	EGR1 MUT F	5' AAC CGG CCC AGC AAG ACA 3'
	EGR1 WT F	5' CTC GTG CTT TAC GGT ATC G 3'
Adamts19$^{-/-}$ **(Adamts19tm4a(EUCOMM)Wtsi)**	Adamts19_244_F	5' AGA AGG GAA CAA ACA CAA CAA GTG 3'
	Adamts19_244_R	5' AGT TAG CCT GAG CCT GTG TGG 3'
	CAS_R1_Term	5' TCG TGG TAT CGT TAT GCG GCC 3'
Mfrp$^{-/-}$ **(B6.C3Ga-Mfrprd6/J)**	Mfrp F	5' CAC TAC CAC CCC AGC AAG GAC 3'
	Mfrp R	5' CTT CTC CAG AGA GTG CCC TTG 3'
Irbp$^{-/-}$ **(B6.129P2-Rbp3tm1Gil/J)**	Common IRBP	5' CAT ATC CAC ACC TGC CAA CA 3'
	MF IRBP	5' GCT ACT TCC ATT TGT CAC GTC C 3'
	WT IRBP	5' GGA CCC ACA CCT GAA GAC AG3'
Ubc-Cre **(C57Bl/6.Cg-Tg(UBC-Cre/ERT2)1Ejb)**	Cr1	5' TGA TGA GGT TCG CAA GAA CC 3'
	Cr2	5' CCA TGA GTG AAC GAA CCT GG 3'

Table S2. List of qPCR primers

Gene	Forward Primer	Reverse Primer
House Keeping Genes		
Actb	5' CCCTGAGGAGCACCCTGTGC 3'	5' GGCTGGGGTGTTGAAGGTCT 3'
Hprt1	5' TGCCGAGGATTTGGAAAAAGTGT 3'	5' GTGATGGCCTCCCATCTCCT 3'
Mapk1	5' TTGAACAGGCTCTGGCCCAC 3'	5' TGAATGGCGCTTCAGCAATGG 3'
Genes of Interest		
Prss56	5' ACCTGGACGCCCTAGACCTC 3'	5' TGTTGGCAACGCCTTGATGT 3'
Adamts19	5' `TGCTGAAGACAACGGCCTGA 3'	5' CAGCACAGGATGGGTGGTCA 3'
Adamts19 Ex3	5' GAGGACTTCCTATTCATTGAGCCA 3'	5' CCTGTATAAACGGTGCGGGT 3'